Preprints of the 19th World Congress
The International Federation of Automatic Control
Cape Town, South Africa. August 24-29, 2014

Observability Analysis of 3D AUV Trimming Trajectories in the Presence of Ocean Currents using Single Beacon Navigation

N. Crasta [*] **M. Bayat** [**] **A. Pedro Aguiar** [**,***]
António M. Pascoal [**,****]

[*] *Institute for Automation and Systems Engineering, Technische Universität Ilmenau, 98684 Ilmenau, Germany.*
[**] *Laboratory of Robotics and Systems in Engineering and Science (LARSyS), IST/University of Lisbon, Av. Rovisco Pais, 1, 1049-001, Lisbon, Portugal.*
[***] *Faculty of Engineering, University of Porto (FEUP), Rua Dr. Roberto Frias, s/n, 4200-465 Porto, Portugal.*
[****] *Adjunct Scientist, National Institute of Oceanography (NIO), Dona Paula, 403004, Goa, India.*

Abstract: This paper addresses the observability properties of a 3D autonomous underwater vehicle (AUV) model in the presence of ocean currents, under the assumption that the vehicle can only measure its distance to a fixed transponder using an acoustic ranging device. In the set-up adopted, the AUV may undergo a wide range of maneuvers that are usually described as *trimming trajectories*. The latter are of paramount importance in flight dynamics and can be completely parametrized by three variables: i) linear body speed v, ii) flight-path angle γ, and iii) yaw rate $\dot{\psi}$. We assume that $v > 0$, γ, and $\dot{\psi}$ are constant but otherwise arbitrary (within the constraints of the vehicle capabilities) and examine the observability of the resulting system with the output (measured) variable described above. We adopt weaker definitions of observability that are akin to those proposed by Herman and Krener (Hermann and Krener, 1977) but reflect the fact that we consider specific kinds of maneuvers in 3D. We show that in the presence of known constant ocean currents the 3D kinematic model of the AUV that corresponds to trimming trajectories with nonzero flight path angle and yaw rate is observable. In case the latter conditions fail, we give a complete characterization of the sets of states that are indistinguishable from a given initial state. We further show that in the case of unknown constant ocean currents the model is locally weakly observable for yaw rate different from zero but fails to be locally weakly observable for zero yaw rate. In both the cases we give a complete characterization of the sets of states that are indistinguishable from a given initial state.

Keywords: Autonomous underwater vehicle (AUV), Single beacon navigation, Range-only measurements, Trimming trajectories, Set of indistinguishable states, Observability.

1. INTRODUCTION

There is currently widespread interest in the development and operation of autonomous robots at sea. Their applications are numerous and encompass a vast number of commercial and scientific missions. Central to the operation of these vehicles is the availability of systems capable of yielding good estimates of their positions underwater. To this effect, a wide range of sensor suites and methods can be used. See for example (Kinsey et al., 2006) and the references therein for a fast paced introduction to this challenging area of research and some of the key technological solutions adopted.

In recent years, motivated by the need to substantially reduce the cost of underwater positioning systems, there has been a flurry of activity on the study of single beacon (SB) positioning systems. The latter have the potential to drastically reduce the complexity of position systems, for they enable a vehicle to find its position in 3D by using only measurements of the successive ranges between the vehicle and a transponder located at a fixed, known position. In spite of significant advances in this area, however much work remains to be done to clarify basic issues related to the observability properties of SB positioning systems. Namely, to characterize the types of vehicle trajectories that render a range-based positioning design model observable. Clearly, this is an important first step in the design of a reliable position estimator.

The literature on SB positioning, oftentimes referred to as single beacon navigation (SBN), is by now quite extensive and defies a simple summary. Different types of models for 2D and 3D SBN navigation systems have been proposed and the corresponding observability issues have been addressed by resorting to a number of methods that include linearization techniques (Gadre and Stilwell, 2004)-(Gadre and Stilwell, 2005) as well as geometric (Filippo et al., 2011) and algebraic methods (Jouffroy and Reger, 2006).

In (Gadre and Stilwell, 2004) the authors study the observability of SBN systems for underwater vehicles evolving in 2D. The nonlinear system is linearized about nomi-

⋆ This work was supported in part by projects MORPH (EU FP7 under grant agreement No. 288704), CONAV/FCT-PT (PTDC/EEA-CRO/113820/2009), and the FCT [PEst-OE/EEI/LA0009/2011].

Copyright © 2014 IFAC

nal trajectories and standard linear time-varying (LTV) observability tools are used to analyze the observability properties of the resulting linear model. In (Gadre and Stilwell, 2005), unknown constant ocean currents are augmented into the state vector and a procedure identical to that in (Gadre and Stilwell, 2004) is used to study the observability of the ensuing model. Because of the tools used, all results are local in nature.

The work in (Filippo et al., 2011) addresses observability issues in the context of relative AUV positioning using inter-vehicle range measurements. This is done by exploiting nonlinear observability concepts and using Herman-Krener observability rank conditions of local weak observability (Hermann and Krener, 1977). The results obtained are validated experimentally in an equivalent SB navigation scenario. In (Jouffroy and Reger, 2006), the authors study the problem of estimating the position of an underwater vehicle using a single acoustic transponder. The proposed estimator structure and related observability conditions are derived using a nonlinear differential algebraic methods. Simple simulation results illustrate the approach adopted. In (Gianfranco et al., 2012) authors address the problem of relative localization of two vehicles with distance between them as measurements.

Recently, in (Bayat and Aguiar, 2012) observability issues in the context of Simultaneous Localization and Mapping (SLAM) of an AUV equipped with inertial sensors, a depth sensor, and an acoustic ranging device that provides relative range measurements to a number of stationary beacons is investigated. For trimming trajectories, it is shown that the set of indistinguishable states from a given initial state with the knowledge of either one of the beacon positions or the AUV position, contains only the zero vector, with the exception of a distinctive case where there is an additional isolated point.

In spite of the progress done towards understanding observability issues related to range-based AUV positioning, work is still required to characterize explicitly the types of AUV trajectories that yield global observability. This is a direct consequence of the nonlinear characteristics of the problem at hand, which mandate the use of analysis tools that go beyond those afforded by the theory of observability for linear time invariant (LTI) systems.

Nonlinear observability theory has received considerably impetus from the pioneering work of (Hermann and Krener, 1977), where the author presented the celebrated Herman-Krener rank condition for local weak observability. Recall that this is a sufficient condition for observability. When the rank condition fails, the observability of the system must be examined in detail. Notice, however that given an initial unobservable state of the system under study, the theory exposed in (Hermann and Krener, 1977) does not provide information about the set of states that are indistinguishable from it. The latter, as is well known, is defined as the set of initial states that produce, for every admissible input, output time-histories identical to those obtained when the system is initiated at the particular unobservable state (Hermann and Krener, 1977). We recall that when the nonlinear system is locally weakly observable at a given initial state in the sense of Herman-Krener, then there exists, for every state in an open neighborhood of the given initial state, a corresponding input that will distinguish it from that given state. Notice, however that this does not imply the existence of a single admissible input that will be able to do so. Hence, practically, there is a need to identify a class of admissible inputs with the property that every input has the ability to distinguish every pair of initial configurations through the outputs.

Motivated by the above considerations, in this paper we analyze the observability properties of a 3D underwater vehicle model the presence of ocean currents, under the assumption that the vehicle can only measure the distance to a fixed transponder located at a known position using an acoustic ranging device. We consider the case where the vehicle moves along trimming trajectories characterized by constant linear body speed, flight path angle, and yaw rate. The latter correspond to helices that can degenerate into straight lines and circumferences. In this paper, we introduce a weaker notion of observability to study the observability of the 3D kinematic model. We show that in the presence of known constant ocean currents the 3D kinematic model of the AUV that corresponds to trimming trajectories with nonzero flight path angle and yaw rate is observable. In case the latter conditions fail, we give a complete characterization of the sets of states that are indistinguishable from a given initial state. We further show that in the case of unknown constant ocean currents the model is locally weakly observable for yaw rate different from zero but fails to be locally weakly observable for zero yaw rate. The proofs of these results are essentially geometric in nature, and depart from common approaches to study the observability of similar systems available in the literature. The envisioned impact of the results is twofold: i) they afford practitioners rules for the choice of general types of trajectories that a vehicle should undergo in order to enhance SB observability properties, and ii) by providing a complete characterization of the sets of indistinguishable states, they may be extremely helpful during the phase of positioning system design by clarifying the number of models to adopt in a multiple model adaptive estimation (MMAE) set-up, along the lines proposed in (Bayat and Aguiar, 2012).

The organization of the paper is as follows. Section 2 introduces some basic notation and mathematical results that will be used in later sections. Section 3 summarizes key definitions of observability in the context of nonlinear systems. Section 4 describes the model adopted for the study of the observability properties of a 3D AUV model when the vehicle moves along trimming trajectories. In the subsequent section we analyze the observability properties of the 3D SB system for the trimming trajectories. Finally, Section 6 discusses the results obtained and introduces some topics that warrant further research effort.

2. MATHEMATICAL PRELIMINARIES

Given $a, b \in \mathbb{R}$ such that $a^2 + b^2 \neq 0$, $\operatorname{atan2}(b, a)$ denotes the unique angle $\theta \in [0, 2\pi)$ satisfying $\sin(\theta) = a/\sqrt{a^2+b^2}$ and $\cos(\theta) = b/\sqrt{a^2+b^2}$. We denote the Euclidean norm in $\mathbb{R}^3$ by $\|\cdot\|$, the unit sphere in $\mathbb{R}^3$ by $\mathrm{S}^2 := \{\boldsymbol{x} \in \mathbb{R}^3 \colon \|\boldsymbol{x}\| = 1\}$, and the 3×3 identity matrix by I_3. We further denote the elements of the standard bases for $\mathbb{R}^3$ by $\boldsymbol{e}_1, \boldsymbol{e}_2$, and $\boldsymbol{e}_3$. The group of special orthogonal matrices in 3-dimensions is represented by SO(3). For every $u \in \mathbb{R}^3$, $(u\times)$ is the matrix representation of the linear map $v \mapsto u \times v$, $v \in \mathbb{R}^3$. Given $u \in \mathbb{R}^3$ and $\theta \in [0, 2\pi)$, $R(u, \theta) \in \mathrm{SO}(3)$ denotes the rotation matrix about the axis u by an angle θ. Given $u \in \mathrm{S}^2$ and $\theta \in \mathbb{R}$, we have (Murray et al., 1994)

$$R(u, \theta) = I_3 + \sin(\theta)\,(u\times) + (1 - \cos(\theta))(u\times)^2.$$

3. OBSERVABILITY OF NONLINEAR SYSTEMS

Consider the nonlinear control system

$$\dot{\boldsymbol{x}} = \boldsymbol{f}(\boldsymbol{x}, \boldsymbol{u}), \quad \boldsymbol{y} = \boldsymbol{h}(\boldsymbol{x}), \tag{3.1}$$

where $\boldsymbol{x} \in \mathbb{R}^n$ is the state, $\boldsymbol{u}$ is the input vector taking values in a compact subset Ω of $\mathbb{R}^p$ containing zero in its interior, $\boldsymbol{f}$ is a complete and smooth vector field on $\mathbb{R}^n$, and the output function $\boldsymbol{h} : \mathbb{R}^n \to \mathbb{R}^q$ has smooth components. We recall the following definitions from (Hermann and Krener, 1977).

Definition 3.1. Two initial states $\boldsymbol{z}, \boldsymbol{z}' \in \mathbb{R}^n$ of (3.1) are *indistinguishable* in $[0, t_f]$ if, for every admissible input $\boldsymbol{u}$, the solutions of (3.1) satisfying the initial conditions $\boldsymbol{x}(0) = \boldsymbol{z}$ and $\boldsymbol{x}(0) = \boldsymbol{z}'$ produce identical output-time histories in $[0, t_f]$. □

For every $\boldsymbol{z} \in \mathbb{R}^n$, let $\mathcal{I}(\boldsymbol{z}) \subseteq \mathbb{R}^n$ denote the set of all states that are indistinguishable from $\boldsymbol{z}$. Note that indistinguishability is an equivalence relation.

Definition 3.2. The system (3.1) is *observable at* $\boldsymbol{z} \in \mathbb{R}^n$ if $\mathcal{I}(\boldsymbol{z}) = \{\boldsymbol{z}\}$, and is *observable* if $\mathcal{I}(\boldsymbol{z}) = \{\boldsymbol{z}\}$ for every $\boldsymbol{z} \in \mathbb{R}^n$. □

Definition 3.3. The system (3.1) is *locally weakly observable at* $\boldsymbol{z} \in \mathbb{R}^n$ if $\boldsymbol{z}$ is an isolated point of $\mathcal{I}(\boldsymbol{z})$ and is *locally weakly observable* if it is locally weakly observable at every $\boldsymbol{z} \in \mathbb{R}^n$. □

We next define a weaker notion of observability.

Definition 3.4. For a given admissible input $\boldsymbol{u}^*$, we say that two initial states $\boldsymbol{z}, \boldsymbol{z}' \in \mathbb{R}^n$ of (3.1) are $\boldsymbol{u}^*$-*indistinguishable* in $[0, t_f]$, if the solutions of (3.1) satisfying the initial conditions $\boldsymbol{x}(0) = \boldsymbol{z}$ and $\boldsymbol{x}(0) = \boldsymbol{z}'$ produce identical output-time histories in $[0, t_f]$ for $\boldsymbol{u}^*$. □

For every $\boldsymbol{z} \in \mathbb{R}^n$, let $\mathcal{I}^{\boldsymbol{u}^*}(\boldsymbol{z}) \subseteq \mathbb{R}^n$ denote the set of all states that are $\boldsymbol{u}^*$-indistinguishable from $\boldsymbol{z}$.

Definition 3.5. The system (3.1) is $\boldsymbol{u}^*$-*observable at* $\boldsymbol{z} \in \mathbb{R}^n$ if $\mathcal{I}^{\boldsymbol{u}^*}(\boldsymbol{z}) = \{\boldsymbol{z}\}$, and is *observable* if $\mathcal{I}^{\boldsymbol{u}^*}(\boldsymbol{z}) = \{\boldsymbol{z}\}$ for every $\boldsymbol{z} \in \mathbb{R}^n$. □

Definition 3.6. The system (3.1) is *locally weakly* $\boldsymbol{u}^*$-*observable at* $\boldsymbol{z} \in \mathbb{R}^n$ if $\boldsymbol{z}$ is an isolated point of $\mathcal{I}^{\boldsymbol{u}^*}(\boldsymbol{z})$ and is *locally weakly* $\boldsymbol{u}^*$-*observable* if it is locally weakly $\boldsymbol{u}^*$-observable at every $\boldsymbol{z} \in \mathbb{R}^n$. □

Remark 3.7. Note that observability (O) implies local weak observability (LWO), while $\boldsymbol{u}^*$-observability ($\boldsymbol{u}^*$-O) implies local weak $\boldsymbol{u}^*$-observability ($\boldsymbol{u}^*$-LWO).

Also note that one can easily derive the observability properties of the system in the sense of Herman-Krener from this weaker notion of observability. In the rest of the paper, we adopt the weaker definitions of observability.

4. 3D SB MODEL AND TRIMMING TRAJECTORIES

In what follows, $\{I\}$ and $\{B\}$ denote a inertial and a body-fixed frame with unit vectors $\{\boldsymbol{x}_I, \boldsymbol{y}_I, \boldsymbol{z}_I\}$ and $\{\boldsymbol{x}_B, \boldsymbol{y}_B, \boldsymbol{z}_B\}$, respectively. See figure (1). We describe the attitude of an AUV using a matrix $R \in \mathrm{SO}(3)$ such that the multiplication of R by a body-fixed vector expresses that vector in the inertial frame. We use the Euler angles of roll (ϕ), pitch (θ), and yaw (ψ) to locally parametrize the rotation matrix R. The kinematic equations that describe the motion of an AUV in $\{I\}$ are given by

$$\dot{\boldsymbol{p}} = R_z(\psi)\, R_y(\theta)\, R_x(\phi)\, \boldsymbol{v} \text{ and } \dot{\boldsymbol{\eta}} = J(\boldsymbol{\eta})\, \boldsymbol{\omega} \tag{4.1}$$

where $\boldsymbol{p} \in \mathbb{R}^3$ is the inertial position of the AUV, $\boldsymbol{v} := (u, v, w) \in \mathbb{R}^3$ is the body-fixed linear velocity vector relative to $\{I\}$ and expressed in $\{B\}$, $\boldsymbol{\omega} := (p, q, r) \in \mathbb{R}^3$ is the body-fixed angular velocity vector relative to $\{I\}$ and

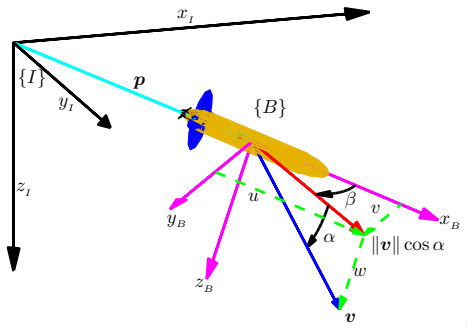

Fig. 1. 3D AUV model for single beacon navigation.

expressed in $\{B\}$, $\boldsymbol{\eta} := (\phi, \theta, \psi) \in [0, 2\pi) \times (-\pi/2, \pi/2) \times [0, 2\pi)$ is the Euler angle vector (roll, pitch, and yaw), $R_z(\psi) = \mathrm{e}^{(\boldsymbol{e}_3\times)\psi}$, $R_y(\theta) = \mathrm{e}^{(\boldsymbol{e}_2\times)\theta}$, $R_x(\phi) = \mathrm{e}^{(\boldsymbol{e}_1\times)\phi}$, and

$$J(\boldsymbol{\eta}) := \begin{bmatrix} 1 & \sin(\phi)\tan(\theta) & \cos(\phi)\tan(\theta) \\ 0 & \cos(\phi) & -\sin(\phi) \\ 0 & \sin(\phi)/\cos(\theta) & \cos(\phi)/\cos(\theta) \end{bmatrix}.$$

Following standard nomenclature (Fossen, 1994), the AUV dynamic equations admit the general representation

$$M \begin{bmatrix} \dot{\boldsymbol{v}} \\ \dot{\boldsymbol{\omega}} \end{bmatrix} + C(\boldsymbol{v}, \boldsymbol{\omega}) \begin{bmatrix} \boldsymbol{v} \\ \boldsymbol{\omega} \end{bmatrix} + D(\boldsymbol{v}, \boldsymbol{\omega}) \begin{bmatrix} \boldsymbol{v} \\ \boldsymbol{\omega} \end{bmatrix} + g(\boldsymbol{\eta}) = \boldsymbol{\tau}, \tag{4.2}$$

where $M := M_{RB} + M_A$ is the generalized mass matrix of the AUV with M_{RB} and M_A denoting the rigid body mass matrix and added mass matrix, respectively, $C(\boldsymbol{v}, \boldsymbol{\omega}) := C_{RB}(\boldsymbol{v}, \boldsymbol{\omega}) + C_A(\boldsymbol{v}, \boldsymbol{\omega})$ is the coriolis and centripetal acceleration matrix, $D(\boldsymbol{v}, \boldsymbol{\omega})$ is the total hydrodynamic damping matrix, $g(\boldsymbol{\eta})$ is the static force and torque vector (due to the interplay between gravity and buoyancy), and $\boldsymbol{\tau}$ is the generalized force vector that includes the external force and torque acting on the AUV, the hydrodynamics force and torque vector (due to viscous damping), and controlled force and torque vector (due to the thrusters and/or control planes).

We now recall the concept of trimming trajectories for a vehicle with motion described by (4.1)-(4.2), see (Elgersma, 1988). This type of trajectories play an important role in the analysis of flight dynamics (namely in aircraft control) because they are the trajectories that correspond to a force-moment equilibrium in the body-fixed frame, for a fixed input control configuration. Mathematically, they correspond to the equilibrium points of the dynamic equation (4.2) with constant inputs, that is, $\dot{\boldsymbol{v}} \equiv \boldsymbol{0}$ and $\dot{\boldsymbol{\omega}} \equiv \boldsymbol{0}$ for all $t \geq 0$, yielding $\boldsymbol{v} = \boldsymbol{v}_{\mathrm{e}}$ and $\boldsymbol{\omega} = \boldsymbol{\omega}_{\mathrm{e}}$, where $\boldsymbol{v}_{\mathrm{e}}$ and $\boldsymbol{\omega}_{\mathrm{e}}$ (values at equilibrium) are constant.

From the dynamic equation (4.2), it follows that all the forces and moments that depend on the linear and rotational velocity vector are constant, with the exception of the static forces and moments $g(\boldsymbol{\eta})$ that depends on ϕ and θ. Hence, for a given constant input configuration, in order to ascertain the balancing of (4.2) it is necessary that $g(\boldsymbol{\eta})$ must be a constant vector, as the linear and angular velocity vectors are constant along the trimming trajectories. Now notice that stationarity of $g(\boldsymbol{\eta})$ implies that ϕ and θ are constant, that is, $\phi = \phi_{\mathrm{e}}$ and $\theta = \theta_{\mathrm{e}}$, where ϕ_{e} and θ_{e} (values at equilibrium) are constant.

At equilibrium $\dot{\phi} = \dot{\phi}_{\mathrm{e}} = 0$ and $\dot{\theta} = \dot{\theta}_{\mathrm{e}} = 0$, thus implying that $\dot{\boldsymbol{\eta}} = \dot{\psi}\, \boldsymbol{e}_3$. Equation (4.1) can be re-written as $\boldsymbol{\omega} = J(\boldsymbol{\eta})^{-1}\, \dot{\boldsymbol{\eta}}$, from which we may conclude that

$$\boldsymbol{\omega}_{\mathrm{e}} = \dot{\psi}\, [-\sin(\theta_{\mathrm{e}}) \;\; \sin(\phi_{\mathrm{e}})\cos(\theta_{\mathrm{e}}) \;\; \cos(\phi_{\mathrm{e}})\cos(\theta_{\mathrm{e}})]^{\mathrm{T}}. \tag{4.3}$$

Notice that the body-fixed trimming angular velocity vector depend on roll, pitch, and yaw rate. Further, since $\boldsymbol{\omega}_{\mathrm{e}}$ is a constant vector, equation (4.3) implies that $\dot{\psi}$ is

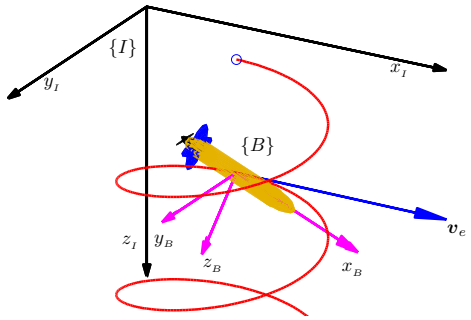

Fig. 2. An AUV trimming trajectory.

a constant. In other words, the trimming yaw angle ψ_e is given by $\psi_e(t) = \dot{\psi}_e\, t + \psi_0$ where $\dot{\psi}_e \in \mathbb{R}$ is the constant yaw rate and $\psi_0 \in [0, 2\pi)$ is the initial yaw angle.

Define $\boldsymbol{\xi} := [\xi_1\ \xi_2\ \xi_3]^{\mathrm{T}} = R_y(\theta_e)R_x(\phi_e)\,\boldsymbol{v}_e$ and note that $\boldsymbol{\xi} \in \mathbb{R}^3$ is a constant vector because $\theta_e, \phi_e, \boldsymbol{v}_e$ are constant. Then, from (4.1), it follows that

$$\dot{\boldsymbol{p}}_e = \begin{bmatrix} \xi_1\cos(\psi_e(t)) + \xi_2\sin(\psi_e(t)) \\ \xi_1\sin(\psi_e(t)) - \xi_2\cos(\psi_e(t)) \\ \xi_3 \end{bmatrix} \tag{4.4}$$

where $\boldsymbol{p}_e$ denotes the trimming position. Define $\psi_v, \gamma \in [0, 2\pi)$ by

$$\psi_v := \mathrm{atan2}(\xi_2, \xi_1) \ \text{ and } \ \gamma := \mathrm{atan2}(-\xi_3, \|\boldsymbol{\xi} \times \boldsymbol{e}_3\|). \tag{4.5}$$

It can be shown that ψ_v is the angle between the vehicle's heading and the velocity vector heading (or, equivalently, *side-slip angle*) and γ is the *trimming flight path angle*. Since $\|\boldsymbol{\xi} \times \boldsymbol{e}_3\| \geq 0$, from (4.5) we conclude that $\gamma \in [-\pi/2, \pi/2]$. Further, we assume that $\|\boldsymbol{\xi} \times \boldsymbol{e}_3\| > 0$, and hence $\gamma \in (-\pi/2, \pi/2)$.

Equation (4.4) is usually written in the equivalent form

$$\dot{\boldsymbol{p}}_e = \|\boldsymbol{v}_e\| \begin{bmatrix} \cos(\gamma)\cos(\psi_e(t) - \psi_v) \\ \cos(\gamma)\sin(\psi_e(t) - \psi_v) \\ -\sin(\gamma) \end{bmatrix}, \tag{4.6}$$

where $\|\boldsymbol{v}_e\|$ is the linear trimming body speed. The solution of (4.6) for the initial condition $\boldsymbol{p}_0 \in \mathbb{R}^3$ is given by

$$\boldsymbol{p}_e(t) - \boldsymbol{p}_0 = \|\boldsymbol{v}_e\|\dot{\psi}_e^{-1}\cos(\gamma) \begin{bmatrix} \sin(\psi_e(t) - \psi_v) - \sin(\psi_e(0) - \psi_v) \\ -\cos(\psi_e(t) - \psi_v) + \cos(\psi_e(0) - \psi_v) \\ -\tan(\gamma)\, t \end{bmatrix},$$

from which it can be easily concluded that the only trimming trajectories of the underwater vehicle are helices with radii $\|\boldsymbol{v}_e\|\,\dot{\psi}_e^{-1}\cos(\gamma)$ that may degenerate into straight lines or circumferences. Thus, all trimming trajectories can be parametrized by total vehicle speed, flight path angle, and yaw rate. See figures 2-3.

In the presence of a constant ocean current $\boldsymbol{v}_c \in \mathbb{R}^3$, equation (4.6) becomes

$$\dot{\boldsymbol{p}}_e = \|\boldsymbol{v}_e\| \begin{bmatrix} \cos(\gamma)\cos(\psi_e(t) - \psi_v) \\ \cos(\gamma)\sin(\psi_e(t) - \psi_v) \\ -\sin(\gamma) \end{bmatrix} + \boldsymbol{v}_c$$

where ψ_v denotes now the angle between the vehicle heading and the heading of the velocity with respect to the fluid. We remark that in the analysis that follows the dynamics of the AUV do not play any role. They were introduced to simply show what kind of trimming trajectories an AUV admits in 3D.

5. OBSERVABILITY ANALYSIS OF SBN

From the results in the previous section, the 3D kinematic model associated with the trimming trajectories of an

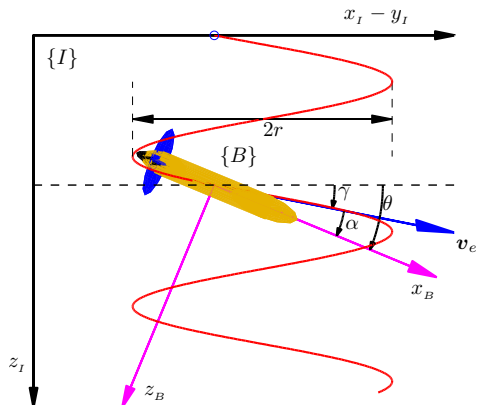

Fig. 3. Trimming trajectory shown in $x_B - z_I$ plane. (γ - flight path angle; θ - pitch angle; α - angle of attack)

AUV measuring its distance to a single transponder, located at a known position vector $\boldsymbol{p}_b \in \mathbb{R}^3$, is given by [1]

$$\left.\begin{aligned} \dot{\boldsymbol{p}}_e(t) &= \boldsymbol{g}(\boldsymbol{v}_e, \gamma, \psi_e, \psi_v, t) + \boldsymbol{v}_c(t), \\ \dot{\boldsymbol{v}}_c(t) &= \boldsymbol{0}, \\ y(t) &= \|\boldsymbol{p}_e(t) - \boldsymbol{p}_b\|, \end{aligned}\right\} \tag{5.1}$$

where

$$\boldsymbol{g}(\boldsymbol{v}_e, \gamma, \psi_e, \psi_v, t) := \|\boldsymbol{v}_e\| \begin{bmatrix} \cos(\gamma)\cos(\dot{\psi}_e t + \psi_0 - \psi_v) \\ \cos(\gamma)\sin(\dot{\psi}_e t + \psi_0 - \psi_v) \\ -\sin(\gamma) \end{bmatrix}, \tag{5.2}$$

$\boldsymbol{p}_e(t) \in \mathbb{R}^3$ is the inertial position vector, $\boldsymbol{v}_c(t) \in \mathbb{R}^3$ a constant ocean current disturbance, $\|\boldsymbol{v}_e\| > 0$ is the linear trimming body speed, $\gamma \in (-\pi/2, \pi/2)$ is the trimming flight path angle, ψ_0 is the initial yaw angle, $\dot{\psi}_e$ is the constant yaw rate and ψ_v is the side-slip angle. Without loss of generality, we assume that the beacon is at the origin.

The solution of (5.1) for the initial condition $(\boldsymbol{x}_0, \boldsymbol{v}_{c_0}) \in \mathbb{R}^3 \times \mathbb{R}^3$ at $t \geq 0$ is denoted by $\Phi_t(\boldsymbol{x}_0, \boldsymbol{v}_{c_0})$ and is given by

$$\Phi_t(\boldsymbol{x}_0, \boldsymbol{v}_{c_0}) = \begin{bmatrix} \boldsymbol{x}_0 \\ \boldsymbol{v}_{c_0} \end{bmatrix} + \begin{bmatrix} \boldsymbol{v}_{c_0}\, t + \int_0^t \boldsymbol{g}(\boldsymbol{v}_e, \gamma, \psi_e, \psi_v, \tau)\,\mathrm{d}\tau \\ \boldsymbol{0} \end{bmatrix},$$

while the output at $t \geq 0$ is given by

$$h(\Phi_t(\boldsymbol{x}_0, \boldsymbol{v}_{c_0})) = \|\boldsymbol{p}_e(t)\|\,.$$

Given $\gamma \in (-\pi/2, \pi/2)$ and $\psi_0, \psi_v \in [0, 2\pi)$, define $t \mapsto \boldsymbol{\kappa}_1, \boldsymbol{\kappa}$ by

$$\boldsymbol{\kappa}(t) := \boldsymbol{\kappa}_0 + \boldsymbol{\kappa}_1(t), \tag{5.3}$$

where

$$\boldsymbol{\kappa}_0 := [-\cos(\gamma)\sin(\psi_0 - \psi_v) \quad \cos(\gamma)\cos(\psi_0 - \psi_v) \quad 0]^{\mathrm{T}}, \tag{5.4}$$

$$\boldsymbol{\kappa}_1(t) := \begin{bmatrix} \cos(\gamma)\sin(\dot{\psi}_e t + \psi_0 - \psi_v) \\ -\cos(\gamma)\cos(\dot{\psi}_e t + \psi_0 - \psi_v) \\ -\dot{\psi}_e\, t\sin(\gamma) \end{bmatrix}. \tag{5.5}$$

It can be shown that

$$\boldsymbol{\kappa}_1^{(j)}(t)\Big|_{t=0} = (\dot{\psi}_e)^j\,\boldsymbol{\zeta}_j,\ 1 \leq j \leq 3, \tag{5.6}$$

where $\boldsymbol{\kappa}_1^{(j)}(t)$ is the jth time derivative of $\boldsymbol{\kappa}_1$ and

$$\begin{aligned} \boldsymbol{\zeta}_1 &:= \cos(\gamma)\,[\cos(\psi_0 - \psi_v) \quad \sin(\psi_0 - \psi_v) \quad -\tan(\gamma)]^{\mathrm{T}}, \\ \boldsymbol{\zeta}_2 &:= \cos(\gamma)\,[-\sin(\psi_0 - \psi_v) \quad \cos(\psi_0 - \psi_v) \quad 0]^{\mathrm{T}}, \\ \boldsymbol{\zeta}_3 &:= \cos(\gamma)\,[\cos(\psi_0 - \psi_v) \quad \sin(\psi_0 - \psi_v) \quad 0]^{\mathrm{T}}. \end{aligned}$$

Further, it can be shown that $\boldsymbol{\kappa}_1^{(4)}(t) = -(\dot{\psi}_e)^2\,\boldsymbol{\kappa}_1^{(2)}(t)$, and as a consequence, all the higher order time derivatives are redundant.

In this paper we study the observability properties of model (5.1) for two distinct cases, namely, *i*) Known ocean

[1] Recall that the observability properties of (5.1) with range squared and range measurement are equivalent (Crasta et al., 2013).

current and *ii*) Unknown ocean current. In the following sections, we characterize the set of indistinguishable states for cases $(i)-(ii)$. Notice that the observability properties depend on the type of trimming trajectory adopted, that is, we first fix a trajectory and examine the observability of the resulting model in (5.1).

5.1 Known Ocean Currents

Consider the system in the presence of a known current $\boldsymbol{v}_{\rm c} \in \mathbb{R}^3$, that is,

$$\dot{\boldsymbol{p}}_{\rm e} = \boldsymbol{g}(\boldsymbol{v}_{\rm e}, \gamma, \boldsymbol{\psi}_{\rm e}, \psi_v, t) + \boldsymbol{v}_{\rm c}, \quad y = \|\boldsymbol{p}_{\rm e}\|^2, \tag{5.7}$$

where $\boldsymbol{g}(\cdot)$ is given by (5.2). Given $\boldsymbol{x} \in \mathbb{R}^3$, we let $\mathcal{I}_2^{\rm z}(\boldsymbol{x})$ and $\mathcal{I}_2^{\rm nz}(\boldsymbol{x})$ denote the set of indistinguishable states from the given initial state $\boldsymbol{x}$ for zero yaw rate and nonzero constant yaw rate, respectively, for the system (5.7). We next characterize $\mathcal{I}_2^{\rm z}(\boldsymbol{x})$ and $\mathcal{I}_2^{\rm nz}(\boldsymbol{x})$.

Zero yaw rate In this case, $\dot{\psi}_{\rm e} = 0$. Then, for a given $\gamma \in (-\pi/2, \pi/2)$, $\psi_0, \psi_v \in [0, 2\,\pi)$ and initial state $\boldsymbol{x} \in \mathbb{R}^3$,

$$\Phi_t(\boldsymbol{x}) = \boldsymbol{x} + \boldsymbol{b}_{\rm tot}(\boldsymbol{v}_{\rm e}, \gamma, \psi_0, \psi_v)\, t,$$

where

$$\boldsymbol{b}_{\rm tot}(\boldsymbol{v}_{\rm e}, \gamma, \psi_0, \psi_v) := \|\boldsymbol{v}_{\rm e}\| \begin{bmatrix} \cos(\gamma)\,\cos(\psi_0 - \psi_v) \\ \cos(\gamma)\,\sin(\psi_0 - \psi_v) \\ -\sin(\gamma) \end{bmatrix} + \boldsymbol{v}_{\rm c}.$$

Proposition 5.1. Consider $\boldsymbol{v}_{\rm c} \in \mathbb{R}^3$, $\|\boldsymbol{v}_{\rm e}\| > 0$, $\gamma \in (-\pi/2, \pi/2)$, and $\psi_0, \psi_v \in [0, 2\,\pi)$. Then, for every $\boldsymbol{x} \in \mathbb{R}^3$,

$$\mathcal{I}_2^{z}(\boldsymbol{x}) = \{\boldsymbol{z} = R(\boldsymbol{b}_{\rm tot}(\boldsymbol{v}_{\rm e}, \gamma, \psi_0, \psi_v), \theta)\, \boldsymbol{x} \colon \theta \in \mathbb{R}\}.$$

Proof. Consider $\boldsymbol{x} \in \mathbb{R}^3$ and let $\boldsymbol{z} \in \mathbb{R}^3$ be such that $\boldsymbol{z} \in \mathcal{I}_2^{\rm z}(\boldsymbol{x})$. Then $h(\Phi_t(\boldsymbol{z})) = h(\Phi_t(\boldsymbol{x}))\ \forall\, t \geq 0$, which implies $\|\boldsymbol{z}\|^2 = \|\boldsymbol{x}\|^2$ and $\boldsymbol{z}^{\rm T}\boldsymbol{b}_{\rm tot} = \boldsymbol{x}^{\rm T}\boldsymbol{b}_{\rm tot}$. These two equations imply $\boldsymbol{z} = R(\boldsymbol{b}_{\rm tot}, \theta)\, \boldsymbol{x}$, $\theta \in \mathbb{R}$. The reverse inclusion is trivial. ■

Remark 5.2. The result above shows that for a given $\boldsymbol{x} \in \mathbb{R}^3$ the set of all the points that are obtained by rotating $\boldsymbol{x}$ about the axis $\boldsymbol{b}_{\rm tot}$ through an arbitrary angle $\theta \in \mathbb{R}$ are indistinguishable. □

Nonzero, constant yaw rate In this case, $\dot{\psi}_{\rm e} > 0$. Then for a given $\boldsymbol{x}, \boldsymbol{v}_{\rm c} \in \mathbb{R}^3$, $\gamma \in (-\pi/2, \pi/2)$, and $\psi_0, \psi_v \in [0, 2\,\pi)$,

$$\Phi_t(\boldsymbol{x}) = \boldsymbol{x} + \|\boldsymbol{v}_{\rm e}\|\, \dot{\psi}_{\rm e}^{-1}\, \boldsymbol{\kappa}(t) + \boldsymbol{v}_{\rm c}\, t.$$

Proposition 5.3. Consider $\boldsymbol{v}_{\rm c} \in \mathbb{R}^3$, $\|\boldsymbol{v}_{\rm e}\|, \dot{\psi}_{\rm e} > 0$, $\gamma \in (-\pi/2, \pi/2)$, and $\psi_0, \psi_v \in [0, 2\,\pi)$. Then, for every $\boldsymbol{x} \in \mathbb{R}^3$,

$$\mathcal{I}_2^{\rm nz}(\boldsymbol{x}) = \begin{cases} \{\boldsymbol{x}, -R(\boldsymbol{e}_3, \pi)\boldsymbol{x}\} & \text{if } \sin(\gamma) = \|\boldsymbol{v}_{\rm e}\|^{-1} \boldsymbol{e}_3^{\rm T}\boldsymbol{v}_{\rm c}, \\ \{\boldsymbol{x}\} & \text{otherwise.} \end{cases}$$

Proof. Consider $\boldsymbol{x} \in \mathbb{R}^3$ and let $\boldsymbol{z} \in \mathbb{R}^3$ be such that $\boldsymbol{z} \in \mathcal{I}_2^{\rm nz}(\boldsymbol{x})$. Then $h(\Phi_t(\boldsymbol{z})) = h(\Phi_t(\boldsymbol{x}))$ for all $t \geq 0$, implies that

$$\|\boldsymbol{z}\|^2 - \|\boldsymbol{x}\|^2 + 2(\boldsymbol{z} - \boldsymbol{x})^{\rm T} \left\{ \|\boldsymbol{v}_{\rm e}\|\, \dot{\psi}_{\rm e}^{-1} \boldsymbol{\kappa}(t) + \boldsymbol{v}_{\rm c} t \right\} = 0. \tag{5.8}$$

At $t = 0$, (5.8) yields $\|\boldsymbol{z}\|^2 = \|\boldsymbol{x}\|^2$. Consequently, (5.8) yields $(\boldsymbol{z} - \boldsymbol{x})^{\rm T} \left\{ \|\boldsymbol{v}_{\rm e}\|\, \dot{\psi}_{\rm e}^{-1} \boldsymbol{\kappa}(t) + \boldsymbol{v}_{\rm c}\, t \right\} = 0$, which upon differentiating with respect to t and evaluating at $t = 0$ along with (5.6) yields

$$\begin{bmatrix} \{\|\boldsymbol{v}_{\rm e}\|\, \boldsymbol{\zeta}_1 + \boldsymbol{v}_{\rm c}\}^{\rm T} \\ \boldsymbol{\zeta}_2^{\rm T} \\ \boldsymbol{\zeta}_3^{\rm T} \end{bmatrix} (\boldsymbol{z} - \boldsymbol{x}) = 0. \tag{5.9}$$

Define $\delta := \|\boldsymbol{v}_{\rm e}\|^{-1} \boldsymbol{e}_3^{\rm T}\boldsymbol{v}_{\rm c}$. From (5.9), it can be easily verified that $\boldsymbol{z} = \boldsymbol{x}$ if and only if $\sin(\gamma) \neq \|\boldsymbol{v}_{\rm e}\|^{-1}\, \boldsymbol{e}_3^{\rm T}\boldsymbol{v}_{\rm c}$. If $\sin(\gamma) = \delta$, then $\boldsymbol{z} \in \{\boldsymbol{x}, -R(\boldsymbol{e}_3, \pi)\boldsymbol{x}\}$ and $\mathcal{I}_2^{\rm nz}(\boldsymbol{x}) \subseteq \{\boldsymbol{x}, -R(\boldsymbol{e}_3, \pi)\boldsymbol{x}\}$. The reverse inclusion is trivial. ■

Remark 5.4. System (5.7) with nonzero flight path angle is observable for every nonzero, constant yaw rate. □

Remark 5.5. By setting $\boldsymbol{v}_{\rm c} = \boldsymbol{0}$, in the above analysis, we obtain the results corresponding to the case where there are no currents. □

5.2 Unknown Ocean Currents

Consider the system in the presence of an unknown constant ocean current $\boldsymbol{v}_{\rm c} \in \mathbb{R}^3$ described by

$$\dot{\boldsymbol{p}}_{\rm e} = \boldsymbol{g}(\boldsymbol{v}_{\rm e}, \gamma, \boldsymbol{\psi}_{\rm e}, \psi_v, t) + \boldsymbol{v}_{\rm c},\ \dot{\boldsymbol{v}}_{\rm c} = \boldsymbol{0},\ y = \|\boldsymbol{p}_{\rm e}\|^2, \tag{5.10}$$

where $\boldsymbol{g}(\cdot)$ is given by (5.2). Given $(\boldsymbol{x}, \boldsymbol{v}_{\rm c}) \in \mathbb{R}^3 \times \mathbb{R}^3$, we let $\mathcal{I}_3^{\rm z}(\boldsymbol{x}, \boldsymbol{v}_{\rm c})$ and $\mathcal{I}_3^{\rm nz}(\boldsymbol{x}, \boldsymbol{v}_{\rm c})$ denote the set of indistinguishable states from the given initial state $(\boldsymbol{x}, \boldsymbol{v}_{\rm c})$ for zero yaw rate and nonzero constant yaw rate, respectively. We next characterize $\mathcal{I}_3^{\rm z}(\boldsymbol{x}, \boldsymbol{v}_{\rm c})$ and $\mathcal{I}_3^{\rm nz}(\boldsymbol{x}, \boldsymbol{v}_{\rm c})$.

Zero yaw rate In this case, $\dot{\psi}_{\rm e} = 0$. Then, for a given initial condition $(\boldsymbol{x}, \boldsymbol{v}_{\rm c}) \in \mathcal{M} := \mathbb{R}^3 \times \mathbb{R}^3$, $\Phi_t(\boldsymbol{x}, \boldsymbol{v}_{\rm c}) = \boldsymbol{x} + \boldsymbol{b}_{\rm tot}(\boldsymbol{v}_{\rm e}, \gamma, \psi_0, \psi_v, \boldsymbol{v}_{\rm c})\, t$, where

$$\boldsymbol{b}_{\rm tot}(\boldsymbol{v}_{\rm e}, \gamma, \psi_0, \psi_v, \boldsymbol{v}_{\rm c}) := \|\boldsymbol{v}_{\rm e}\|\, \hat{u}(\gamma, \psi_0, \psi_v) + \boldsymbol{v}_{\rm c}, \tag{5.11}$$

$$\hat{u} := \begin{bmatrix} \cos(\gamma)\cos(\psi_0 - \psi_v) & \cos(\gamma)\sin(\psi_0 - \psi_v) & -\sin(\gamma) \end{bmatrix}^{\rm T}.$$

Proposition 5.6. Consider $\|\boldsymbol{v}_{\rm e}\| > 0$, $\gamma \in (-\pi/2, \pi/2)$, and $\psi_0, \psi_v \in [0, 2\pi)$. Define

$$u(\boldsymbol{\mu}) := [\sin(\mu_1)\cos(\mu_2)\ \ \sin(\mu_1)\sin(\mu_2)\ \ \cos(\mu_1)]^{\rm T},$$

with $\boldsymbol{\mu} := (\mu_1, \mu_2) \in \mathcal{A} := [0, \pi] \times [0, 2\pi]$. Then, for a given $(\boldsymbol{x}, \boldsymbol{v}_{\rm c}) \in \mathcal{M}$,

$$\mathcal{I}_3^{z}(\boldsymbol{x}, \boldsymbol{v}_{\rm c}) = \{(\|\boldsymbol{x}\|\, u(\boldsymbol{\mu}), -\|\boldsymbol{v}_{\rm e}\|\, \hat{u} + \|\boldsymbol{v}_{\rm t}\|\, u(\boldsymbol{\sigma})) : (\boldsymbol{\mu}, \boldsymbol{\sigma}) \in \mathcal{Q}\},$$

where $\boldsymbol{v}_{\rm t} := \|\boldsymbol{v}_{\rm e}\|\, \hat{u} + \boldsymbol{v}_{\rm c}$, $\cos(\lambda) := \left(\|\boldsymbol{x}\|^{-1}\boldsymbol{x}\right)^{\rm T} \left(\|\boldsymbol{v}_{\rm t}\|^{-1}\boldsymbol{v}_{\rm t}\right)$, and $\mathcal{Q} := \left\{(\boldsymbol{\mu}, \boldsymbol{\sigma}) \in \mathcal{A} \times \mathcal{A} \colon u(\boldsymbol{\mu})^{\rm T} u(\boldsymbol{\sigma}) = \cos(\lambda)\right\}$.

Proof. Consider $(\boldsymbol{x}, \boldsymbol{v}_{\rm c}) \in \mathcal{M}$ and let $(\boldsymbol{z}, \boldsymbol{w}_{\rm c}) \in \mathcal{M}$ be such that $(\boldsymbol{z}, \boldsymbol{w}_{\rm c}) \in \mathcal{I}_3^{\rm z}(\boldsymbol{x}, \boldsymbol{v}_{\rm c})$. Then $h(\Phi_t(\boldsymbol{z}, \boldsymbol{w}_{\rm c})) = h(\Phi_t(\boldsymbol{x}, \boldsymbol{v}_{\rm c}))$ for all $t \geq 0$ implies that

$$\|\boldsymbol{z}\|^2 = \|\boldsymbol{x}\|^2,\ \ \|\boldsymbol{w}_{\rm t}\|^2 = \|\boldsymbol{v}_{\rm t}\|^2,\ \ \boldsymbol{z}^{\rm T}\boldsymbol{w}_{\rm t} = \boldsymbol{x}^{\rm T}\boldsymbol{v}_{\rm t}, \tag{5.12}$$

where $\boldsymbol{w}_{\rm t} := \|\boldsymbol{v}_{\rm e}\|\, \hat{u} + \boldsymbol{w}_{\rm c}$ and $\boldsymbol{v}_{\rm t} := \|\boldsymbol{v}_{\rm e}\|\, \hat{u} + \boldsymbol{v}_{\rm c}$. Equation (5.12) implies that

$$\boldsymbol{z} = \|\boldsymbol{x}_0\|\, u(\boldsymbol{\mu}),\ \ \boldsymbol{w}_{\rm c} = -\|\boldsymbol{v}_{\rm e}\|\, \hat{u}(\gamma, \psi_0, \psi_v) + \|\boldsymbol{v}_{\rm t}\|\, u(\boldsymbol{\sigma}), \tag{5.13}$$

with $(\boldsymbol{\mu}, \boldsymbol{\sigma}) \in \mathcal{A} \times \mathcal{A}$. Using (5.13) in (5.12), we have $(\boldsymbol{\mu}, \boldsymbol{\sigma}) \in \mathcal{Q}$ and hence $\mathcal{I}_3^{\rm z}(\boldsymbol{x}, \boldsymbol{v}_{\rm c}) \subseteq \{(\|\boldsymbol{x}\|\, u(\boldsymbol{\mu}), -\|\boldsymbol{v}_{\rm e}\|\, \hat{u} + \|\boldsymbol{v}_{\rm t}\|\, u(\boldsymbol{\sigma})) : (\boldsymbol{\mu}, \boldsymbol{\sigma}) \in \mathcal{Q}\}$. Conversely, consider $\boldsymbol{q} = (\boldsymbol{q}_1, \boldsymbol{q}_2)$ where $\boldsymbol{q}_1 = \|\boldsymbol{x}\| u(\boldsymbol{\mu})$ and $\boldsymbol{q}_2 = -\|\boldsymbol{v}_{\rm e}\| \hat{u} + \|(\|\boldsymbol{v}_{\rm e}\|\, \hat{u} + \boldsymbol{v}_{\rm c})\|\, u(\boldsymbol{\sigma})$ for some $(\boldsymbol{\mu}, \boldsymbol{\sigma}) \in \mathcal{Q}$. Using the properties of the rotation matrices, it can be shown that $h(\Phi_t(\boldsymbol{q})) = h(\Phi_t(\boldsymbol{x}, \boldsymbol{v}_{\rm c}))$ for all $t \geq 0$. Hence, the result follows. ■

Remark 5.7. The result above shows that for a given $(\boldsymbol{x}, \boldsymbol{v}_{\rm c}) \in \mathcal{M}$ the set of all the points that are indistinguishable from $(\boldsymbol{x}, \boldsymbol{v}_{\rm c})$ is a 3 dimensional manifold. Hence, the system is not locally weakly observable. □

Nonzero, constant yaw rate In this case, $\dot{\psi}_{\rm e} > 0$. Then, for a given $\boldsymbol{z} := (\boldsymbol{x}, \boldsymbol{v}_{\rm c})$, we have $\Phi_t(\boldsymbol{z}) = \boldsymbol{x} + \|\boldsymbol{v}_{\rm e}\|\, \dot{\psi}_{\rm e}^{-1}\, \boldsymbol{\kappa}(t) + \boldsymbol{v}_{\rm c}\, t$.

Proposition 5.8. Consider $\|\boldsymbol{v}_{\rm e}\| > 0$, $\psi_0, \psi_v \in [0, 2\,\pi)$ and $\gamma \in (-\pi/2, \pi/2)$. Then, for a given $\boldsymbol{z} = (\boldsymbol{x}, \boldsymbol{v}_{\rm c}) \in \mathcal{M}$,

$$\mathcal{I}_3^{\rm nz}(\boldsymbol{z}) = \left\{\boldsymbol{z}, (-R(\boldsymbol{e}_3, \pi)\boldsymbol{x}, 2\|\boldsymbol{v}_{\rm e}\| \sin(\gamma)\boldsymbol{e}_3 - R(\boldsymbol{e}_3, \pi)\boldsymbol{v}_{\rm c})\right\}.$$

Proof. Consider $(\boldsymbol{x}_1, \boldsymbol{v}_{\rm c_1}) \in \mathcal{M}$ and let $(\boldsymbol{x}_2, \boldsymbol{v}_{\rm c_2}) \in \mathcal{M}$ be such that $(\boldsymbol{x}_2, \boldsymbol{v}_{\rm c_2}) \in \mathcal{I}_3^{\rm nz}(\boldsymbol{x}_1, \boldsymbol{v}_{\rm c_1})$. Then $h(\Phi_t(\boldsymbol{x}_2, \boldsymbol{v}_{\rm c_2})) =$

$h(\Phi_t(\boldsymbol{x}_1, \boldsymbol{v}_{c_1}))$ at $t = 0$ implies that $\|\boldsymbol{x}_2\|^2 = \|\boldsymbol{x}_1\|^2$. For every $j \in \{1, 2\}$, define $\boldsymbol{\nu}_j(t) := \|\boldsymbol{v}_e\| \dot{\psi}_e^{-1} \boldsymbol{\kappa}(t) + \boldsymbol{v}_{c_j} t$, and note that $\dot{\boldsymbol{\nu}}_j(t) = \|\boldsymbol{v}_e\| \dot{\psi}_e^{-1} \dot{\boldsymbol{\kappa}}(t) + \boldsymbol{v}_{c_j}$. Consequently, $\ddot{\boldsymbol{\nu}}_1(t) = \ddot{\boldsymbol{\nu}}_2(t) := \|\boldsymbol{v}_e\| \dot{\psi}_e^{-1} \ddot{\boldsymbol{\kappa}}(t)$. Using $\|\boldsymbol{x}_2\|^2 = \|\boldsymbol{x}_1\|^2$ in $h(\Phi_t(\boldsymbol{x}_2, \boldsymbol{w}_{c_2})) = h(\Phi_t(\boldsymbol{x}_1, \boldsymbol{v}_{c_1}))$ we have

$$\|\boldsymbol{\nu}_2(t)\|^2 + 2\,\boldsymbol{x}_2^{\mathrm{T}}\boldsymbol{\nu}_2(t) = \|\boldsymbol{\nu}_1(t)\|^2 + 2\,\boldsymbol{x}_1^{\mathrm{T}}\boldsymbol{\nu}_1(t),\ \forall\, t \geq 0. \tag{5.14}$$

The successive time derivatives of (5.14) evaluated at $t = 0$ are given by

$$\boldsymbol{x}_2^{\mathrm{T}}\dot{\boldsymbol{\nu}}_2(0) = \boldsymbol{x}_1^{\mathrm{T}}\dot{\boldsymbol{\nu}}_1(0) \tag{5.15}$$

$$\|\dot{\boldsymbol{\nu}}_2(0)\|^2 + \boldsymbol{x}_2^{\mathrm{T}}\ddot{\boldsymbol{\nu}}_1(0) = \|\dot{\boldsymbol{\nu}}_1(0)\|^2 + \boldsymbol{x}_1^{\mathrm{T}}\ddot{\boldsymbol{\nu}}_1(0) \tag{5.16}$$

$$3\,\dot{\boldsymbol{\nu}}_2(0)^{\mathrm{T}}\ddot{\boldsymbol{\nu}}_2(0) + \boldsymbol{x}_2^{\mathrm{T}}\dddot{\boldsymbol{\nu}}_1(0) = 3\,\dot{\boldsymbol{\nu}}_1(0)^{\mathrm{T}}\ddot{\boldsymbol{\nu}}_1(0) + \boldsymbol{x}_1^{\mathrm{T}}\dddot{\boldsymbol{\nu}}_1(0) \tag{5.17}$$

$$4\,\dot{\boldsymbol{\nu}}_2(0)^{\mathrm{T}}\dddot{\boldsymbol{\nu}}_2(0) + \boldsymbol{x}_2^{\mathrm{T}}\ddot{\boldsymbol{\nu}}_1(0) = 4\,\dot{\boldsymbol{\nu}}_1(0)^{\mathrm{T}}\dddot{\boldsymbol{\nu}}_1(0) + \boldsymbol{x}_1^{\mathrm{T}}\ddot{\boldsymbol{\nu}}_1(0) \tag{5.18}$$

$$5\,\dot{\boldsymbol{\nu}}_2(0)^{\mathrm{T}}\ddot{\boldsymbol{\nu}}_2(0) + \boldsymbol{x}_2^{\mathrm{T}}\dddot{\boldsymbol{\nu}}_1(0) = 5\,\dot{\boldsymbol{\nu}}_1(0)^{\mathrm{T}}\ddot{\boldsymbol{\nu}}_1(0) + \boldsymbol{x}_1^{\mathrm{T}}\dddot{\boldsymbol{\nu}}_1(0) \tag{5.19}$$

$$6\,\dot{\boldsymbol{\nu}}_2(0)^{\mathrm{T}}\dddot{\boldsymbol{\nu}}_2(0) + \boldsymbol{x}_2^{\mathrm{T}}\boldsymbol{\nu}_1^{(2)}(0) = 6\,\dot{\boldsymbol{\nu}}_1(0)^{\mathrm{T}}\dddot{\boldsymbol{\nu}}_1(0) + \boldsymbol{x}_1^{\mathrm{T}}\ddot{\boldsymbol{\nu}}_1(0). \tag{5.20}$$

Equations (5.17) and (5.19) imply that

$$\dot{\boldsymbol{\nu}}_2(0)^{\mathrm{T}}\ddot{\boldsymbol{\nu}}_2(0) = \dot{\boldsymbol{\nu}}_1(0)^{\mathrm{T}}\ddot{\boldsymbol{\nu}}_1(0), \tag{5.21}$$

while (5.18) and (5.20) yield

$$\dot{\boldsymbol{\nu}}_2(0)^{\mathrm{T}}\dddot{\boldsymbol{\nu}}_2(0) = \dot{\boldsymbol{\nu}}_1(0)^{\mathrm{T}}\dddot{\boldsymbol{\nu}}_1(0). \tag{5.22}$$

Since $\ddot{\boldsymbol{\nu}}_2(0) = \ddot{\boldsymbol{\nu}}_1(0)$ and $\dddot{\boldsymbol{\nu}}_2(0) = \dddot{\boldsymbol{\nu}}_1(0)$, equations (5.21)-(5.22) imply that

$$\dot{\boldsymbol{\nu}}_2(0) - \dot{\boldsymbol{\nu}}_1(0) = \alpha\,(\ddot{\boldsymbol{\nu}}_2(0) \times \dddot{\boldsymbol{\nu}}_2(0)),\ \alpha \in \mathbb{R}. \tag{5.23}$$

Note that

$$\ddot{\boldsymbol{\nu}}_2(0) = \|\boldsymbol{v}_e\|\,\dot{\psi}_e\,\cos(\gamma)\,\begin{bmatrix}-\sin(\psi_0 - \psi_v) & \cos(\psi_0 - \psi_v) & 0\end{bmatrix}^{\mathrm{T}},$$

$$\dddot{\boldsymbol{\nu}}_2(0) = -\|\boldsymbol{v}_e\|\,\dot{\psi}_e^2\,\cos(\gamma)\,\begin{bmatrix}\cos(\psi_0 - \psi_v) & \sin(\psi_0 - \psi_v) & 0\end{bmatrix}^{\mathrm{T}},$$

and therefore

$$\ddot{\boldsymbol{\nu}}_2(0) \times \dddot{\boldsymbol{\nu}}_2(0) = (\|\boldsymbol{v}_e\|\,\cos(\gamma))^2\ \dot{\psi}_e^3\,\boldsymbol{e}_3 \neq 0. \tag{5.24}$$

Further, it can be easily verified that

$$\boldsymbol{e}_3^{\mathrm{T}}\ddot{\boldsymbol{\nu}}_2(0) = \boldsymbol{e}_3^{\mathrm{T}}\dddot{\boldsymbol{\nu}}_2(0) = 0. \tag{5.25}$$

Using (5.24) in (5.23) yields

$$\dot{\boldsymbol{\nu}}_2(0) = \dot{\boldsymbol{\nu}}_1(0) + \alpha\,(\|\boldsymbol{v}_e\|\cos(\gamma))^2\,(\dot{\psi}_e)^3\boldsymbol{e}_3,\ \alpha \in \mathbb{R}. \tag{5.26}$$

Using (5.25) and (5.26) in (5.17)-(5.18) gives

$$\ddot{\boldsymbol{\nu}}_1(0)^{\mathrm{T}}(\boldsymbol{x}_2 - \boldsymbol{x}_1) = 0 \,\text{and}\, \dddot{\boldsymbol{\nu}}_1(0)^{\mathrm{T}}(\boldsymbol{x}_2 - \boldsymbol{x}_1) = 0. \tag{5.27}$$

Using the above equation along with $\|\boldsymbol{x}_2\|^2 = \|\boldsymbol{x}_1\|^2$ we may conclude that $\boldsymbol{x}_2 \in \{\boldsymbol{x}_1,\ -R(\boldsymbol{e}_3, \pi)\boldsymbol{x}_1\}$. Using the fact that $\dot{\boldsymbol{\nu}}_2(0) = \dot{\boldsymbol{\nu}}_1(0) + \alpha\,[\|\boldsymbol{v}_e\|\,\cos(\gamma)]^2\,\dot{\psi}_e^3\,\boldsymbol{e}_3,\ \alpha \in \mathbb{R}$, we can conclude that

$$\mathcal{I}_3^{\mathrm{nz}}(\boldsymbol{x}, \boldsymbol{v}_c) \subseteq \{(\boldsymbol{x}, \boldsymbol{v}_c), (\boldsymbol{x}, 2\|\boldsymbol{v}_e\|\sin(\gamma)\boldsymbol{e}_3 - R(\boldsymbol{e}_3, \pi)\boldsymbol{v}_c),$$
$$(-R(\boldsymbol{e}_3, \pi)\boldsymbol{x}, \boldsymbol{v}_c), (-R(\boldsymbol{e}_3, \pi)\boldsymbol{x}, 2\|\boldsymbol{v}_e\|\sin(\gamma)\boldsymbol{e}_3 - R(\boldsymbol{e}_3, \pi)\boldsymbol{v}_c)\}.$$

The reverse inclusion is trivial. ■

Remark 5.9. The system (5.10) with nonzero constant yaw rate is locally weakly observable, but not globally observable. □

Tables 1 and 2 summarizes the results in the weaker notion of observability defined in the Section 3 and in the Hermann-Krener sense, respectively. [2]

System	Zero yaw rate	Nonzero, constant yaw rate	
		$\sin(\gamma) = \boldsymbol{e}_3^{\mathrm{T}}\boldsymbol{v}_c$	$\sin(\gamma) \neq \boldsymbol{e}_3^{\mathrm{T}}\boldsymbol{v}_c$
No current	Not $\boldsymbol{u}^*$-LWO	$\boldsymbol{u}^*$-LWO	$\boldsymbol{u}^*$-O
Known current	Not $\boldsymbol{u}^*$-LWO	$\boldsymbol{u}^*$-LWO	$\boldsymbol{u}^*$-O
Unknown current	Not $\boldsymbol{u}^*$-LWO	$\boldsymbol{u}^*$-LWO	$\boldsymbol{u}^*$-LWO

Table 1. Summary of observability analysis with weaker notion.

[2] O: Observable; LWO: Locally weakly observable; $\boldsymbol{u}^*$-O: $\boldsymbol{u}^*$-Observable; $\boldsymbol{u}^*$-LWO: Locally weakly $\boldsymbol{u}^*$-observable

System	Zero yaw rate	Nonzero, constant yaw rate
No current	O	O
Known current	O	O
Unknown current	Not LWO	LWO

Table 2. Summary of observability analysis in the Hermann-Krener sense.

6. CONCLUSIONS

In this paper we introduced a weaker notion of observability to study the observability properties of a 3D kinematic model of an AUV undergoing trimming trajectories and using its distance to a fixed transponder as the output function. With known constant ocean currents (including zero currents), the kinematic model of the AUV that corresponds to trimming trajectories of nonzero flight path angle and nonzero, constant yaw rate were shown to be observable. We showed that, when the former condition fails, the system becomes locally weakly observable. Further, for zero yaw rate, we characterized the set of indistinguishable states from a given initial state, which is a one-dimensional manifold. With unknown currents, for nonzero, constant yaw rate the system becomes locally weakly observable, and for zero yaw rate the system fails to be locally weakly observable. In both the cases we gave an explicit characterization of the set of indistinguishable states from a given initial configuration. Future work will aim at exploiting the use of trimming trajectories to estimate the position of an underwater vehicle in 3D using a SB navigation system.

REFERENCES

M. Bayat and A. P. Aguiar. Observability analysis for AUV range-only localization and mapping: Measures of unobservability and experimental results. In *MCMC IFAC Conference*, 2012.

N. Crasta, M. Bayat, A. P. Aguiar, and A. Pascoal. Observability analysis of the 2D single-beacon navigation with range-only measurements for two classes of maneuvers. In *CAMS IFAC Conference*, 2013.

M. R. Elgersma. *Control of nonlinear systems using partial dynamic inversion.* PhD thesis, University of Minnesota, Minneapolis, MI, USA, 1988.

A. Filippo, A. Gianluca, A. P. Aguiar, and A. M. Pascoal. Observability metric for the relative localization of AUVs based on range and depth measurements: Theory and experiments. In *IROS IEEE/RSJ Conference*, 2011.

T. I. Fossen. *Guidance and control of ocean vehicles.* John Wiley & Sons, 1994.

A. S. Gadre and D. J. Stilwell. Toward underwater navigation based on range measurements from a single localization. In *ICRA IEEE Conference*, 2004.

A. S. Gadre and D. J. Stilwell. Underwater navigation in the presence of unknown currents based on range measurements from a single location. In *American Control Conference*, 2005.

P. Gianfranco, P. Paola, and I. Giovanni. Relative pose observability analysis for 3d nonholonomic vehicles based on range. In *CAMS IFAC Conference*, 2012.

R. Hermann and A. J. Krener. Nonlinear controllability and observability. *IEEE Transactions on Control*, AC-22(5):728–740, October 1977.

J. Jouffroy and J. Reger. An algebraic perspective to single-transponder underwater navigation. In *ICCA IEEE Conference*, 2006.

J. C. Kinsey, R. M. Eustice, and L. L. Whitcomb. A survey of underwater vehicle navigation: Recent advances and new challenges. In *MCMC IFAC Conference*, 2006.

R. M. Murray, Z. Li, and S. S. Sastry. *A Mathematical Introduction to Robotic Manipulation.* Wiley, 1994.